

Study on the formation law of natural gas hydrate under sulfur deposition

Yanhui Ren¹, Lan Tang¹, Yang Wang¹, Yue Gao¹, Meihua Li¹, Chenxi Gao²

¹Southwest oil and gas field company northeast Sichuan gas division, Dazhou, 635000, China

²School of southwest petroleum university, Chengdu, 610500, China

Abstract

Unconventional oil and gas resources are abundant in China, among which high sulfur gas reserves are huge. Exploration and development level of the key to solve the balance between energy supply and demand. In the process of high sulfur natural gas development, studying the formation law of hydrate is the key to ensure the normal operation of pipeline transportation. In this paper, X-ray diffraction was carried out on Si, Sii and SH crystals to explore the growth rate of different crystals in different crystal planes. Conjugate gradient method and Newton-Larson method are used to test the molecular structure of low energy, and the accurate lowest energy conformation of the molecule was obtained. The influence of temperature on hydrate growth was investigated by molecular dynamics simulation method, and the formation process and conditions of hydrate were also obtained. The experimental results show that the polyhedral pores formed by water molecules constantly decompose and recombine, and cannot enter the pores to form stable hydrates under the temperature of 283K. In addition, the stability of hydrogen bonds decreases with the increase of temperature, and the stability of hydrate begins to decline with the increase of temperature, while the crystallinity and order of the system increase with the decrease of temperature. The research in this paper can provide a theoretical basis for the prevention and control of hydrate in high sulfur environment.

Keywords

Molecular dynamics; Hydrate; polyhedral cavity; Newton-Larson method; Conjugate gradient method.

1. Introduction

The molecular mechanism of hydrate nucleation cannot be solved experimentally. the reason is that hydrate nucleation can occur in nanoseconds or tens of nanoseconds, which is not possible in hydrate experiments with such precise timing and location. However, classical molecular dynamics simulations can record molecular motions at the nanosecond level, and it is considered to be the preferred method to study hydrate formation processes.

The basic principle of molecular dynamics is: a suitable model is established based on specific parameters (such as concentration, density, saturation, solubility, etc.) to provide the system with a suitable force field to represent the interaction between the particles in the system. Then set the boundary conditions and initial conditions (e.g. position, pressure, temperature, etc.) according to the specific working conditions, and choose a suitable integration to control the temperature or pressure of the system. Set a reasonable time step and simulation time. After the simulation starts, the system will automatically calculate the energy (such as gravitational potential energy, kinetic potential energy, non-bond energy, electrostatic energy, van der Waals energy, etc.), velocity and position of each particle at each moment, and finally get the development process of the whole system with time through the constant update of time^{[4][5]}.

In this study, molecular dynamics simulations of hydrate nucleation processes were conducted by using Materials Studio (MS) software. Materials Studio is one of the most widely used molecular dynamics simulation software, which contains many functional modules (e.g. Amorphous Cell, Blends, CASTEP, CCDC, DMol3, Forcite, Gaussian, Polymorph, VAMP, etc.) that allow users to build 3D structure models through various The user can build the 3D structure model through various control panels and function modules, and perform various calculations (e.g., energy calculation, geometry optimization, kinetic calculation, annealing simulation, etc.) through the calculation functions under the corresponding modules. In this study, the Amorphous Cell module and the Forcite module are mainly used. The Amorphous Cell module is used to build the model, and the Forcite module is used to perform the calculations and analysis.

2. Molecular dynamics simulation of hydrate formation in the absence of sulfur

2.1. Modeling

Gas hydrates are non-chemometric cage-like crystalline substances composed of water with a molar fraction of about 85% and 15% of guest molecules (e.g., methane, ethane, propane, isobutane, cyclopentane, carbon dioxide, nitrogen, and hydrogen sulfide gas molecules). The water molecules are connected by hydrogen bonds to form polyhedral cage-shaped pores of different sizes, and different guest molecules can be filled in these pores to form different types of gas hydrates with thermodynamic stability, and there are three common crystal types as follows: S I , S II and SH. natural gas hydrates are mainly methane hydrates, and methane hydrates belong to S I type hydrates. According to the X-ray diffraction results, the structural parameters of S I type methane hydrate are obtained as shown in Tables 1 and 2.

Table 1 s | Type I methane hydrate unit cell parameters

Ideal composition	Lattice Type	Space group code	Lattice parameters
(CH ₄) 8 (H ₂ O) 46	body-centered cube (cubic)	Pm3n	11.877Å

Table 2 C, O atomic coordinates

Atom	Oxidation state	x	y	z	Site occupancy
O	-2	0.0000	0.3086	0.1168	1.0
O	-2	0.1835	0.1835	0.1835	1.0
O	-2	0.0000	0.5000	0.2500	1.0
C	-4	0.0000	0.0000	0.0000	1.0
C	-4	0.2500	0.5000	0.0000	1.0

Crystal layer

According to the data in Tables 1 and 2, Build-Crystals in Materials studio in order to build the crystals, then add C and O atoms by Build-Add atoms, and then use the Bernal-Fowler law to add H atoms to C and O atoms to satisfy the The overall net dipole moment is zero. The built methane hydrate cell is shown in Figure 1.

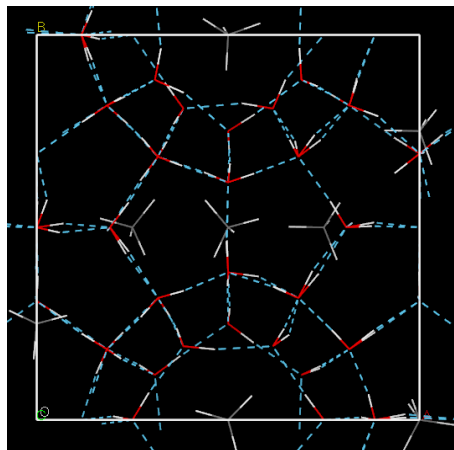


Fig.1 Unit cell of methane hydrate

The growth rates of crystals in different crystal planes are different, and it is shown that s I methane hydrate has the fastest growth rate in the (111) crystal plane. Therefore, the crystal was cut along the (111) crystal plane to build a supercell with the size of $16.797 \text{ \AA} \times 16.797 \text{ \AA} \times 13.714 \text{ \AA}$, as shown in Figure 2.

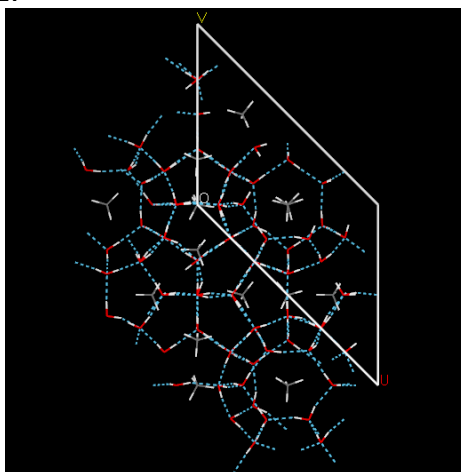


Fig.2 Supercell established along the (111) plane

Solution layer

The ideal composition of s I methane hydrate is $(\text{CH}_4)_8(\text{H}_2\text{O})_{46}$, $\text{CH}_4:\text{H}_2\text{O}=1:5.75$. A solution system containing 115 H_2O molecules and 20 CH_4 molecules is established in this ratio, and the size of the system is $16.797 \text{ \AA} \times 16.797 \text{ \AA} \times 20.118 \text{ \AA}$ with a density of 0.7 g/cm^3 .

Vacuum layer

Since periodic boundary conditions cannot be used in the direction perpendicular to the crystal plane, it is necessary to create a vacuum layer in this direction to eliminate surface and size effects, and the volume of the vacuum layer is $16.797 \text{ \AA} \times 16.797 \text{ \AA} \times 10.000 \text{ \AA}$.

The initial model formed by combining the above 3-layer structure in the manner of crystal layer-solution layer-crystal layer-vacuum layer is shown in Figure 3.

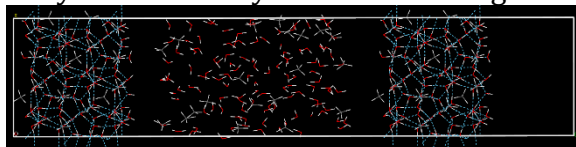


Fig. 3 Initial model without sulfur

2.2. Simulation process

After the model is built, the model needs to be optimized using energy minimization (finding the potential energy minimum) to obtain a model with an optimal structure. The methods

commonly used in molecular mechanics to find the minimum value of potential energy include the fastest descent method, conjugate gradient method, Newton-Larson method, approximate Newton-Larson method, diagonal block Newton-Larson method, etc. Each method has its own advantages, and choosing the appropriate method can speed up the optimization and save more computation time. In this study, the Smart Minimizer method is used - firstly, the low-energy molecular structure is obtained roughly by the fastest descent method, secondly, the true lowest-energy molecular structure is obtained mainly by the conjugate gradient method, and finally, the Newton-Larson method is used to obtain a more accurate lowest-energy conformation of the molecule. The specific optimization parameters are shown in Table 3.

Table 3 Parameter settings of the structural optimization process

Parameter	Force Field	Static seeks	Van der Waals seeks to work with	Cut-off radius	Optimization methods	Number of iteration steps
Setting	cvff	Ewald	Atom based	0.8nm	Smart	10000

Figures 4 and 5 show that the model converges when the optimization proceeds to 1740 steps, at which point the system energy reaches a minimum of -1572.29 kcal/mol.

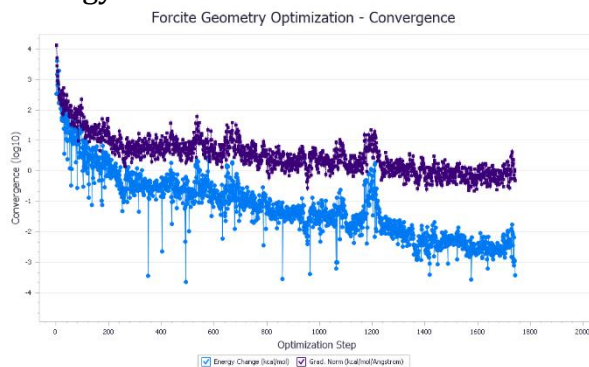


Fig.4 Convergence curve during geometric optimization

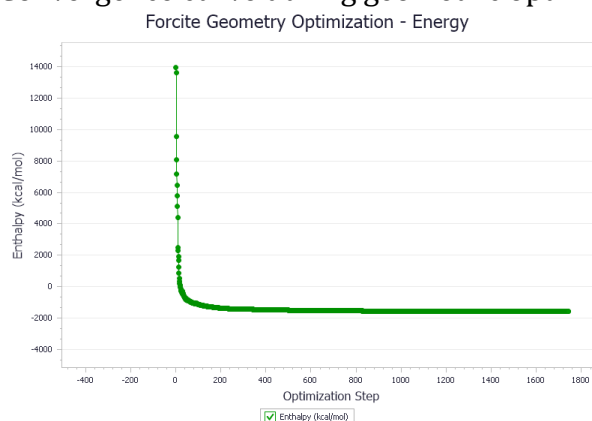


Fig.5 Energy changes during geometry optimization

Taking 263 K as an example, Figures 6 and 7 show the process of system energy as well as temperature change during the kinetic optimization. From the figures, it can be seen that the temperature and energy of the system gradually converge to equilibrium during the 100 ps chirality process.

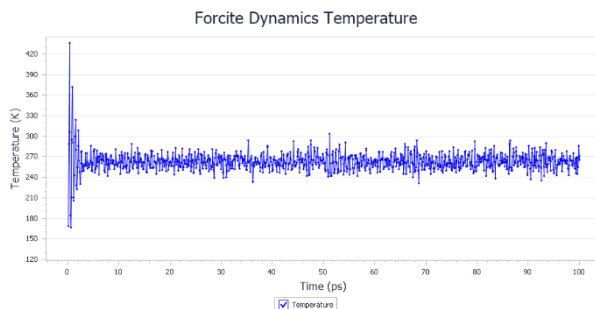


Fig.6 Temperature variation curve during relaxation process

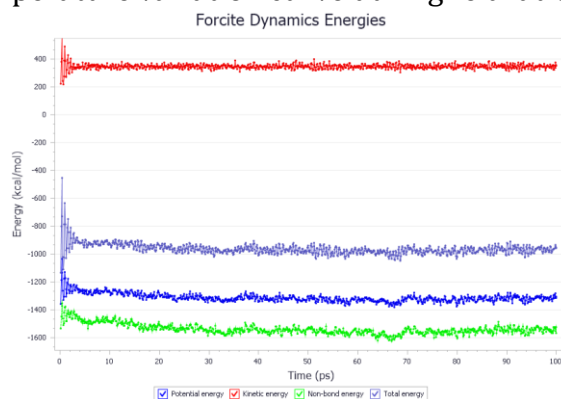


Fig.7 Energy change curve during relaxation process

Subsequently, simulations at different temperatures were performed, and the specific simulation parameters are shown in Table 5 below.

Table 5 Simulation process parameter settings

Parameter	Force Field	Static seeks	Van der Waals seeks to work with	Cut-off radius	System Integration	Constant temperature	Step length	Time
Setting	cvff	Ewald	Atom based	0.8nm	NVT	Nose	1fs	200ns

2.3. Formation process of methane hydrate

It is shown that the hydrate growth process is a phase change process, in which the water-gas mixed liquid phase gradually changes into a water-gas wrapped crystal structure with fixed symmetry, and the hydrate growth process is based on the hydrate crystalline surface and grows gradually to the liquid phase in a layer manner. The hydrate/liquid phase interface is first formed by water molecules to form a semi-crystal cage, and then the guest methane molecules are adsorbed to complete the growth. [11].

Figure 8 shows the conformational changes of the system during the simulation at a temperature of 283 K. It can be seen from the figure that in the beginning, methane molecules are randomly distributed in the water-gas-liquid phase (Figure 8(a)); then, water molecules are connected by hydrogen bonds and form unstable polyhedral pores, and due to the low solubility of methane molecules in water and the supersaturation of methane molecules at this time, methane molecules rapidly aggregate into nanobubbles (Figure 8(b)), and this process is maintained for a long time; in the subsequent simulations, the polyhedral pores formed by water molecules are continuously decomposing and reorganizing without forming a more

obviously shaped hydrate cage, and therefore no methane enters the pores to form stable hydrates.

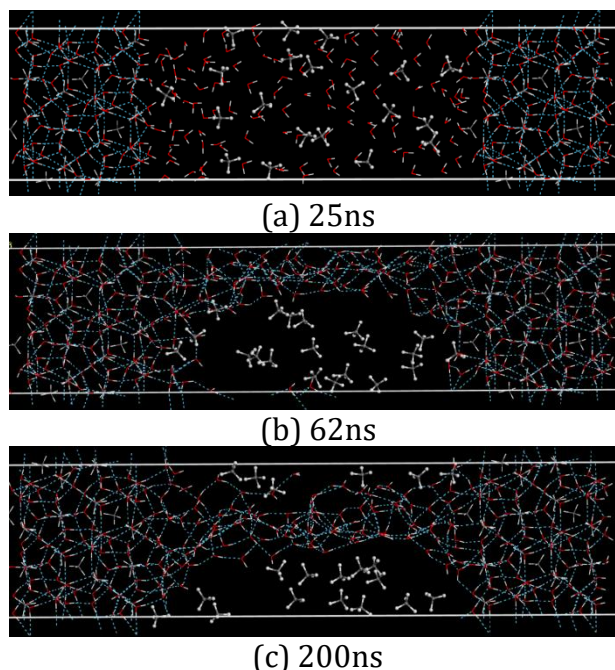


Fig.8 The conformational changes of the system at 283 K during the simulation

2.4. Effect of temperature on hydrate formation

Nucleation of hydrates is studied in the laboratory mainly by macroscopic means such as statistical induction times (minutes to days) and detection of methane consumption. Induction time is the time when hydrate can be detected macroscopically, while nucleation time refers to the time of appearance of the first stable hydrate nucleus in the system, which cannot be accurately determined by macroscopic means and therefore cannot be accurately detected experimentally [12][13].

In this study, the effect of temperature on hydrate nucleation and growth will be investigated microscopically using molecular dynamics simulations in the temperature range of 263-300 K selected at 25 MPa by radial distribution functions.

2.4.1. Radial distribution function analysis

The basic structural feature of methane hydrates is that the main water molecules are connected by hydrogen bonds to form a series of polyhedral pores of different sizes, which are connected by vertices or faces and develop in all directions to form cage hydrates. Therefore, the effect of temperature on methane hydrate formation can be studied by analyzing the stability of hydrogen bonding at different temperatures.

In molecular dynamics simulations, the formation of hydrogen bonds is generally reflected by the radial distribution function (RDF) of O-H in water molecules. The functional expression of the RDF is as follows:

$$g(r) = \frac{1}{4\pi r^2 \delta r \rho} \frac{\sum_{t=1}^T \sum_{j=1}^N \Delta N(r \rightarrow r + \delta r)}{NT}$$

Where N is the total number of particles, T is the total simulation time, δr is the travel distance, and ΔN is the number of particles within this distance.

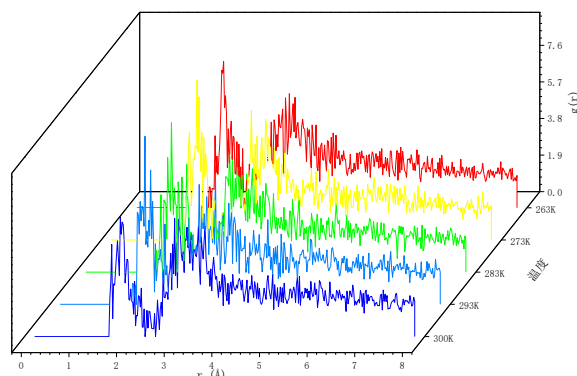


Fig.9 Radial distribution curves of O-H in water molecules at different temperatures

Figure 9 shows the RDF curves of O-H in water molecules at different temperatures for a simulation time of 50s. It can be seen from the figure that the first wave peak of each curve appears near 2.2 Å, which represents hydrogen bonding, and the second wave peak appears near 3.4 Å, which represents no hydrogen bonding. With the increase of temperature, the peak of the first wave decreased obviously, indicating that the stability of hydrogen bonding decreased with the increase of temperature, then the stability of the generated hydrate cage also decreased with the increase of temperature, i.e., the lower the temperature, the higher the crystallinity and orderliness of the system.

3. Conclusion

The conditions of hydrate generation and the effect of temperature on hydrate growth were investigated by using molecular dynamics simulations in a perimetric situation, and the results showed:

- (1) The time required for hydrate generation is long, and the homogeneous solubility model established, cannot form hydrates.
- (2) The temperature is at 283 K because of the low solubility of methane molecules in water. It is not possible to form hydrates at temperature.
- (3) As the temperature increases, the stability of the generated hydrates starts to decrease with the increase in temperature.

Acknowledgements

This work was supported in part by the Sichuan Science and Technology Program (2023YFH0102 and 2022YFH0119), and in part by the scientific research starting project of SWPU (No. 2021QH040).

References

- [1] Cheng Wei dong. The geochemical characteristics of carbonate crusts and sedimentary carbonate minerals in the gas hydrate potential area in the northern South China Sea and their indicative significance [D]. Xiamen University, 2020.
- [2] Chen Yong. Occurrence and magnetic characteristics of iron in sediments of gas hydrate potential areas in the northern South China Sea [D]. Xiamen University, 2019.
- [3] Lin Zhong liang. Characteristics of sediment deposition and iron composition in the gas hydrate potential area in the northern South China Sea and their indicative significance [D]. Xiamen University, 2017.

- [4] Ruppel C D, Kessler J D. The interaction of climate change and methane hydrates[J]. *Reviews of Geophysics*, 2017, 55(1): 126-168.
- [5] Xu W, Ruppel C. Predicting the occurrence, distribution, and evolution of methane gas hydrate in porous marine sediments[J]. *Journal of Geophysical Research: Solid Earth*, 1999, 104(B3): 5081-5095.
- [6] Li Xin. Research progress on industrial application of natural gas hydrate [J]. *Industrial Technology Innovation*, 2020, Vol. 7(1):92-96.
- [7] Lu Hongfeng, Liu Jian, Wu Lushan, Chen Fang, Liao Zhiliang. Sulfur isotopic characteristics of authigenic pyrite in natural gas hydrate boreholes in the South China Sea [J]. *Geoscience Frontiers*, 2015, (2): 200-206.
- [8] Wang Junjie. Comparison of geochemical characteristics of sediments hosted by gas hydrates of different origins in the South China Sea [D]. University of Chinese Academy of Sciences (Guangzhou Institute of Geochemistry, Chinese Academy of Sciences), 2021.
- [9] Deng Yinan, Fang Yunxin, Zhang Xin, Chen Fang, Wang Haifeng, Ren Jiangbo, Liu Chenhui, Guan Yao. The geochemical characteristics of trace elements in the sediments of Qiongdongnan sea area of the South China Sea and their indicative significance for natural gas hydrates [J]. *Marine Geology and Quaternary Geology*, 2017, Volume 37(5): 70-81.
- [10] Lu Yi. Occurrence and evolution characteristics of active silicon in shallow sediments on the northern slope of the South China Sea and its implications for gas hydrate [D]. Xiamen University, 2018.
- [11] Ruppel C. Tapping methane hydrates for unconventional natural gas[J]. *Elements*, 2007, 3(3): 193-199.
- [12] Hesselbo S P, Gröcke D R, Jenkyns H C, et al. Massive dissociation of gas hydrate during a Jurassic oceanic anoxic event[J]. *Nature*, 2000, 406(6794): 392-395.
- [13] Kvenvolden K A. Gas hydrates—geological perspective and global change[J]. *Reviews of geophysics*, 1993, 31(2): 173-187.
- [14] Yao Bochu. Formation conditions and distribution characteristics of natural gas hydrates in the South China Sea [J]. *Offshore Oil*, 2007, Vol. 27(1): 1-10.
- [15] Wu Nengyou, Zhang Guangguang, Liang Jinqiang, et al. Research progress of natural gas hydrate on the northern slope of the South China Sea [J]. *Progress in New Energy*, 2013, (1): 80-94.
- [16] Zhou Hailing. The effect of marine sediment capillary action on the formation and distribution of gas hydrate [D]. Shanghai Ocean University, 2021.